Adsorption (2016) 22:151–158
DOI 10.1007/s10450-015-9732-2

CO_2 capture by Mg–Al and Zn–Al hydrotalcite-like compounds

Thiago M. Rossi[1] · **Juacyara C. Campos**[1] · **Mariana M. V. M. Souza**[1]

Received: 13 June 2015 / Revised: 3 October 2015 / Accepted: 25 November 2015 / Published online: 8 December 2015

Abstract Hydrotalcite-like compounds (HTC) are distinguished by their properties for CO_2 capture, like high surface area, basic sites, thermal stability and good adsorption/desorption efficiency. Mg–Al e Zn–Al HTCs with Al^{3+} molar ratios x = 0.20, 0.28 and 0.33 were synthesized by coprecipitation, and subsequently calcined at 400 °C. For both HTCs, X-ray diffraction patterns have attested the formation of mixed oxides through calcination. The amount of basic sites, measured by temperature-programmed desorption of CO_2, decreases as x increases. The CO_2 adsorption was performed in a thermogravimetric balance using an adsorption temperature of 50 °C. Mg–Al and Zn–Al samples with x = 0.33 molar composition presented the highest CO_2 adsorption, 0.91 and 0.21 mmol g^{-1}, respectively. The Langmuir isotherm fitted well to the experimental data. It was also found that increasing the number of adsorption/desorption cycles the CO_2 adsorption decreases, which is associated with the irreversible chemisorption.

Keywords Hydrotalcite-like compounds · Basic sites · Adsorption · Carbon dioxide

1 Introduction

Human activities are increasingly consuming the world resources and the concern about environmental degradation is more and more part of our society. The growing emission of greenhouse gases is worrying because of the major environmental hazards associated with these emissions. There are many gases causing the greenhouse effect, and carbon dioxide is the main among them. Since the time of the industrial revolution, the atmospheric CO_2 concentration has risen by about 35 % to a value of 400 ppm, and is expected to reach 550 ppm by 2050 even if CO_2 emission is stable for the next four decades (IEA Statistics 2014). Consequently, the planet temperature is rising, causing several environmental impacts. Thus, technologies must be developed in order to prevent or reduce CO_2 emissions.

There are three main approaches for CO_2 separation and capture: membrane purification, liquid absorption and adsorption using solids. Membranes are more promising for concentrated CO_2 streams at elevated pressures (Choi et al. 2009). Amines are the most commonly used liquid absorbent for CO_2 capture and it is a well-established commercial technology (Choi et al. 2009; D'Alessandro et al. 2010). Unlike liquid absorbents, solid adsorbents can be used over a wider temperature range from ambient temperature to 700 °C, yield less waste during cycling, and the spent solids can be disposed of without undue environmental precautions (Wang et al. 2011). Moreover, solid adsorbents exhibit better energy efficiency in the regeneration stage compared with absorption approaches and better chemical stability in presence of hydrogen sulfide and steam (D'Alessandro et al. 2010). The adsorbent must have high CO_2 selectivity and adsorption capacity, fast adsorption/desorption kinetics, stable adsorption capacity after repeated adsorption/desorption cycles, and adequate

Electronic supplementary material The online version of this article (doi:10.1007/s10450-015-9732-2) contains supplementary material, which is available to authorized users.

✉ Mariana M. V. M. Souza
mmattos@eq.ufrj.br

[1] Escola de Química, Universidade Federal do Rio de Janeiro (UFRJ), Centro de Tecnologia, Bloco E, Sala 206, Rio de Janeiro, RJ CEP 21941-909, Brazil

mechanical strength of adsorbent particles after cyclic exposure to high pressure streams (Yong et al. 2001; Yong and Rodrigues 2002). Zeolites, activated carbons, alkaline oxides and hydrotalcite-like compounds are examples of solid adsorbents for CO_2 removal (Choi et al. 2009; D'Alessandro et al. 2010).

Hydrotalcites (HTs) are anionic clays with lamellar structure formed by brucite-like layers [$Mg(OH)_2$], where part of Mg^{2+} is replaced by Al^{3+}, and an interlayer space containing CO_3^{2-} anions and water molecules. Hydrotalcite-like compounds (HTCs), also known as layered double hydroxides (LDHs), are produced by partial or total substitution of Mg^{2+} by other divalent cations and Al^{3+} by other trivalent cations, with similar ionic radius. Equation 1 shows general formula for HTCs (Cavani et al. 1991):

$$\left[M^{2+}_{1-x}M^{3+}_{x}(OH)_2\right]^{x+}\left(A^{n-}_{x/n}\cdot mH_2O\right)^{x-} \quad (1)$$

where: M^{2+} is divalent cation (Mg^{2+}, Ni^{2+}, Zn^{2+}, Cu^{2+}, Mn^{2+}, etc.); M^{3+} is trivalent cation (Al^{3+}, Fe^{3+}, Cr^{3+}, etc.); A^{n-} is the charge compensation anion (CO_3^{2-}, SO_4^{2-}, NO_3^-, Cl^-, OH^-, etc.) and x is the molar ratio of trivalent cation [$M^{3+}/(M^{2+}+M^{3+})$], normally ranging between 0.17 and 0.33.

In general, the CO_2 capture capacities of HTCs are somewhat lower than those of other chemisorbents (typically <1.0 mmol g^{-1}) (Choi et al. 2009); however, the adsorption capacities can be altered substantially by controlling the type and amount of divalent and trivalent cations, and also the thermal treatment. Upon calcination, HTCs gradually lose interlayer water, dehydroxylate and decarbonate, leading to formation of mixed oxides with large surface area and basic sites that enhance CO_2 adsorption. Besides the efforts made to increase the CO_2 capture capacity, another important issue is to enhance the long-term stability of HTCs during adsorption/desorption cycling operation, which is crucial for the development of practical applications (Wang et al. 2011).

Yong and Rodrigues (2002) studied the effect of different divalent cations (Ni, Cu, Co, Zn and Mg) on CO_2 adsorption capacity at 25 °C, showing that Mg–Al sample presented the best value (approximately 0.55 mmol g^{-1}). With regard to this HT, the aluminum content was reported to directly affect the adsorption capacity. The adsorption capacity of Mg–Al sample decreased during about the first 10 cycles of adsorption/desorption under dry or wet conditions. Oliveira et al. (2008) studied three commercial Mg–Al HTs with different Mg/Al ratio and the CO_2 adsorption capacities were lower than 0.1 mmol g^{-1} at 400 °C.

Ram Reddy et al. (2006) reported the effect of calcination temperature on the CO_2 adsorption capacity of Mg–Al HT with x = 0.25. The sample calcined at 400 °C showed the highest adsorption capacity, which was associated with a compromise between the surface area and availability of basic sites. Another parameter varied by Ram Reddy et al. (2006) was the adsorption temperature (100–400 °C), where 200 °C showed the highest adsorption (0.49 mmol g^{-1}). The increase in adsorption temperature (200–400 °C) decreased CO_2 adsorption capacity, because the higher levels of kinetic energy cause CO_2 desorption. On the other hand, at 100 °C there was lack of energy to promote activation of basic sites.

The aim of this paper is to evaluate the CO_2 adsorption capacity of Mg–Al and Zn–Al hydrotalcite-like compounds of different compositions (x = 0.20, 0.28 and 0.33), after calcination, correlating with surface area and amount of basic sites. The choice of two divalent cations aims to study the effect of basicity on CO_2 adsorption; moreover, Zn-based HTCs are less reported in the literature. The CO_2 adsorption equilibrium using Langmuir model and the effect of adsorption/desorption cycles are also presented.

2 Experimental

2.1 Preparation of adsorbents

Mg–Al and Zn–Al HTCs were prepared by coprecipitation method at room temperature based on Corma et al. (1994). 200 mL of solution A, containing nitrate precursors ($Al/(M^{2+}+Al) = 0.20$, 0.28 or 0.33 and $[M^{2+}+Al] = 1.5$ mol L^{-1}, where M^{2+} represents Mg^{2+} or Zn^{2+}), was slowly dropped (1 mL min^{-1}) in a Teflon reactor under vigorous stirring to 200 mL of solution B, containing appropriated amounts of Na_2CO_3 and NaOH ($CO_3^{2-}/Al^{3+} = 0.375$ and $OH^-/Al^{3+} = 6.3$). Following the end of dripping of solution A, the gel formed in the reactor was maintained under agitation for 1 h to complete the precipitation. The suspension was aged in an oven at 60 °C for 18 h. Then, the precipitate was vacuum filtered and washed with deionized water at 90 °C until the filtrate was pH neutral in order to ensure complete removal of the base. The washed precipitate was dried at 110 °C overnight. The mixed oxides were obtained by calcination of the HTCs at 400 °C for 2 h using a heating rate of 10 °C min^{-1} under air flow (60 mL min^{-1}). The samples will be referred to as MgAlXXX or ZnAlXXX, where XXX = 020, 028 or 033, depending on $x = Al/(M^{2+}+Al)$ molar ratio of the synthesis gel.

2.2 Characterization of adsorbents

The chemical composition was determined by X-ray fluorescence (XRF), performed on a Rigaku RIX 3100 spectrometer equipped with rhodium tube.

X-ray powder diffraction (XRD) was performed on a Rigaku Miniflex II diffractometer with graphite monochromator and Cu Kα radiation (30 kV and 15 mA). Analysis was conducted between $2\theta = 5°$ and 90° with steps of 0.05° using a counting time of 2 s by step.

The textural characteristics, such as specific surface area, average pore size and pore size distribution, were investigated from nitrogen physisorption analysis using the Brunauer, Emmett and Teller (BET) and Barrett, Joyner and Hallenda (BJH) methods. The N_2 adsorption and desorption isotherms were measured at −196 °C in a Micromeritics TriStar II 3020 device.

The amount and nature of the basic sites were determined by temperature- programmed desorption of CO_2 (TPD-CO_2), carried out in conventional equipment coupled to a PrismaPlus (Pfeiffer) mass spectrometer. The sample was pretreated at 400 °C for 1 h under He flow (30 mL min^{-1}). CO_2 adsorption was performed under 40 mL min^{-1} of 10 %CO_2/He at room temperature for 30 min; then the sample was treated with He flow for 1 h in order to remove CO_2 physically adsorbed. Finally, TPD profile was recorded when the sample was heated at 20 °C min^{-1} to 700 °C using He as the carrier gas at a flow rate of 40 mL min^{-1}. Relations m/e = 2, 12, 15, 16, 18, 28, 32 and 44 were monitored and m/e = 44 was used for CO_2 quantification.

2.3 Measurements of CO_2 adsorption capacity

CO_2 adsorption capacity was measured by thermogravimetric (TG) analysis using TA SDT-Q600 device. Before the adsorption, in situ heat treatment at 400 °C for 1 h was performed. Then, the sample was cooled to 50 °C, where the CO_2 adsorption was processed. After adsorption, the desorption step was performed heating the sample to 300 °C and then the sample was cooled again to 50 °C. A second adsorption was performed in order to find CO_2 physically adsorbed. Nitrogen flowed at 50 mL min^{-1} in the heat treatment, cooling and desorption. In the adsorption steps a mixture with 10 % CO_2/He flowed at 50 mL min^{-1}. The cooling and heating rates were 2 and 10 °C min^{-1}, respectively.

2.4 CO_2 adsorption isotherms

The experimental CO_2 sorption isotherm experiments were performed on the same TG equipment. Different CO_2 concentrations were obtained diluting a mixture of 10 %CO_2/He with appropriate amounts of He. Firstly, an in situ heat treatment at 400 °C for 1 h was performed. Then, the sample was cooled at 2 °C min^{-1} up to 50 °C, the adsorption temperature.

The CO_2 adsorption isotherms were fitted with a Langmuir model (Eq. 2) and the model was linearized (Eq. 3) to calculate q_m and b parameters:

$$q = \frac{q_m b C}{1 + bC} \tag{2}$$

$$\frac{1}{q} = \frac{1}{q_m b}\frac{1}{C} + \frac{1}{q_m} \tag{3}$$

where q is the CO_2 combined adsorbed amount (mmol CO_2 g^{-1}), q_m is the CO_2 adsorbed amount corresponding to a monolayer (mmol CO_2 g^{-1}), b is the equilibrium constant (L mmol CO_2^{-1}) and C is the CO_2 concentration in CO_2/He mixture (mmol CO_2 L^{-1}).

2.5 CO_2 adsorption/desorption cycles

Three CO_2 adsorption/desorption cycles were evaluated using the same TG apparatus. Firstly, an in situ heat treatment at 400 °C for 1 h was performed. Then, the sample was cooled at 2 °C min^{-1} up to 50 °C, when the first adsorption took place. After adsorption, the desorption was performed at 300 °C under flowing N_2. This procedure was repeated three times. The same flow and heating/cooling rates as described in Sect. 2.3 were used.

3 Results and discussion

3.1 Characterization of adsorbents

The chemical composition of the HTCs is presented in Table 1. The composition of the as-synthesized samples is similar to that of the gel of synthesis, indicating an approximately complete incorporation of the cations in HTC structure.

The XRD patterns of hydrotalcite-like precursors (Fig. 1) exhibit sharp and symmetrical reflections at 11.7°, 23.2°, 60.6° and 61.8° (ascribed to the diffraction by the (003), (006), (110) and (113) planes) and broad and asymmetric reflections at 34.7°, 38.8° and 46.0° (ascribed to the diffraction by the (102), (105) and (108) planes), characteristic of a well-crystallized Mg–Al HT (JCPDS 41-1428) or Zn–Al HTC (JCPDS 38-0486), with rhombohedral symmetry (Silva et al. 2010; León et al. 2010). In this later case, the absence of other phases suggests that Zn^{2+} has isomorphically replaced Mg^{2+} cations in the brucite-like layers.

After calcination at 400 °C, the characteristic lamellar structure disappears by loss of interlayer water, dehydroxylation and decarbonation, which occurs in sequence as temperature increases (Yang et al. 2002). Consequently, the materials become nearly amorphous and XRD patterns (Fig. 2) show the presence of only MgO periclase (JCPDS 45-0946) or ZnO phase (JCPDS 36-1451). These results indicate that aluminum oxide is well dispersed in MgO or ZnO matrix with formation of a solid solution, in

Table 1 Chemical composition and textural characteristics of the adsorbents

Sample	x	Non-calcined			Calcined at 400 °C		
		A_{BET} (m^2 g^{-1})	V_{poro} (cm^3 g^{-1})	D_{poro} (Å)	A_{BET} (m^2 g^{-1})	V_{poro} (cm^3 g^{-1})	D_{poro} (Å)
MgAl020	0.23	92	0.27	120.2	212	0.38	96.2
MgAl028	0.30	54	0.18	140.2	206	0.23	64.2
MgAl033	0.35	76	0.23	117.1	187	0.31	98.7
ZnAl020	0.22	73	0.25	176.9	94	0.30	166.0
ZnAl028	0.31	68	0.23	182.1	82	0.27	176.1
ZnAl033	0.36	91	0.32	167.4	118	0.43	168.8

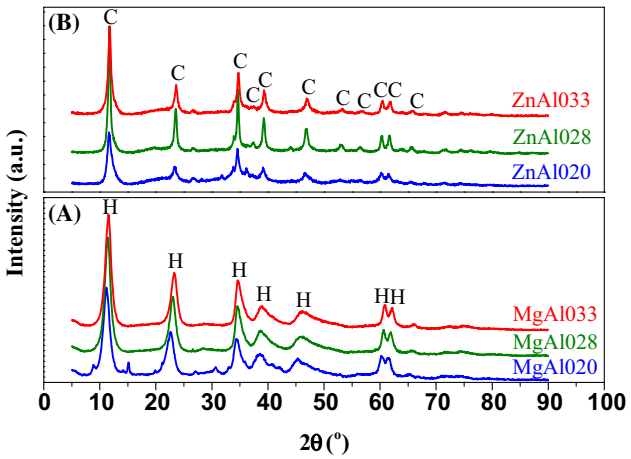

Fig. 1 X-ray diffraction profiles of **a** MgAl and **b** ZnAl HTCs before calcination. H = hydrotalcite ($Mg_6Al_2CO_3(OH)_{16}{\cdot}4H_2O$) and C = Zn and Al hydroxycarbonate ($Zn_6Al_2CO_3(OH)_{16}{\cdot}4H_2O$)

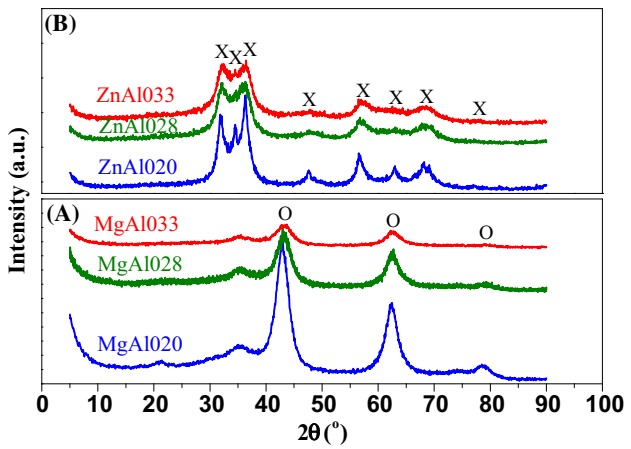

Fig. 2 X-ray diffraction profiles of **a** MgAl and **b** ZnAl after calcination. O = periclase (MgO) and X = zincite (ZnO)

accordance with the literature (Yang et al. 2002; Hutson et al. 2004; Sampieri and Lima 2009; León et al. 2010).

The specific surface area, pore volume and average pore diameter of HTC samples, before and after calcination, are presented in Table 1. Adsorption–desorption isotherms of nitrogen for all samples exhibited the type IV pattern, which are typical of mesoporous solids (pore size between 20 and 500 Å), according to the IUPAC classification (Sing et al. 1985). They all presented H3 hysteresis loop, which is observed with aggregates of plate-like particles giving rise to slit-shaped pores, and is affected by phenomena such as delayed pore condensation, percolation, and pore blocking (Sing et al. 1985; Hutson et al. 2004). After calcination, it was observed an increase in surface area and pore volume, as shown in Table 1, which can be attributed to the elimination of carbonate anions as CO_2, leading to the destruction of the layered structure (as observed by XRD). The strains associated with the resulting 3-D structure and with the compression-expansion of the octahedral layer are related to the significant increase in surface area (Hutson et al. 2004; León et al. 2010).

The non-calcined samples presented similar surface areas, irrespective to the M^{2+} cation. However, after calcination, Mg(Al)O mixed oxides showed much larger surface area than Zn(Al)O samples, as observed by Béres et al. (1999). The obtained values of surface areas are in accordance with others in the literature. Silva et al. (2010) reported BET surface areas of 83 m^2 g^{-1} for Mg–Al HT (x = 0.33) and 202 m^2 g^{-1} after calcination at 400 °C, while the values measured by Abelló et al. (2005) were 57 m^2 g^{-1} for Mg–Al HT (x = 0.22) and 210 m^2 g^{-1} after calcination at 450 °C. For Mg–Al calcined samples, the surface area decreased with increasing Al content (higher values of x), similarly to that observed by Corma et al. (2005): 214 m^2 g^{-1} for x = 0.25, 173 m^2 g^{-1} for x = 0.30 and 162 m^2 g^{-1} for x = 0.33 (samples were calcined at 450 °C).

The basicity of the mixed oxides obtained from HTC calcination was investigated by TPD-CO_2 (Fig. 3). The complex desorption profiles are clearly related to the presence of basic sites with different strengths. For all samples the profiles consist of: (i) a low temperature peak, with maximum desorption at around 120–130 °C, attributed to CO_2 interaction with weak basic sites, (ii) a small desorption peak in the range 170–250 °C, related to medium basic strength sites, and (iii) a large desorption peak at

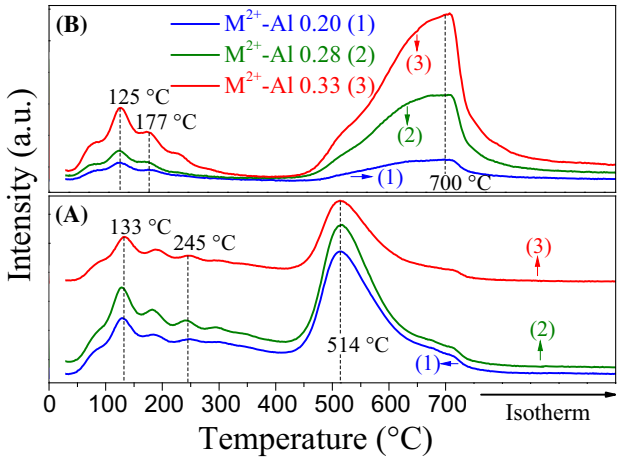

Fig. 3 TPD-CO_2 profiles of **a** MgAl and **b** ZnAl calcined samples

high temperatures (>500 °C), associated with CO_2 desorption from sites of strong basicity. The weak basic sites correspond to OH^- groups on the surface, the medium strength sites are related to the oxygen in both M^{2+}-O^{2-} and Al^{3+}-O^{2-} pairs and the strong basic sites correspond to isolated O^{2-} anions (Di Cosimo et al. 1998; Bolognini et al. 2002; Liu et al. 2014).

A deconvolution procedure using multi-peak Gaussian fitting was applied to TPD-CO_2 profiles and the amount of CO_2 desorbed from each site is shown in Table 2. It can be clearly seen that strong basic sites are predominant over weak and medium basic sites, in accordance with other works in the literature (Di Cosimo et al. 1998; Silva et al. 2010). The amount of basic sites for MgAl HTC found here is much lower than the value reported by Hutson and Attwood (2008) (692 μmol g^{-1} for MgAl with x = 0.25), but their TPD profile did not keep a constant baseline as those presented in Fig. 3. On the other hand, Kustrowski et al. (2004) found by TPD-CO_2 an amount of basic sites of only 46.7 μmol g^{-1} for MgAl HT with x = 0.33, calcined at 600 °C. These same authors reported values of 39.6 μmol g^{-1} for MgAl with x = 0.33, 126.9 μmol g^{-1} for x = 0.25 and 166.7 μmol g^{-1} for x = 0.20, all of them calcined at 450 °C (Kustrowski et al. 2005). These values are close to those calculated in this work.

Table 2 also shows that the total basicity decreases with increasing x and MgAl samples are more basic than ZnAl ones. Using the Sanderson electronegativity model, Rodrigues (2005) showed that the increase on $x = M^{3+}/(M^{2+}+M^{3+})$ ratio in HTCs increases the electronegativity and decreases basicity, as observed experimentally in the present work. Moreover, as electronegativity of Zn^{2+} is higher than Mg^{2+}, ZnAl HTC is expected to have lower basicity than MgAl, as observed by Sampieri and Lima (2009).

3.2 CO_2 adsorption

Table 3 shows the combined, physical and chemical CO_2 adsorption capacities and also reversible fraction for MgAl and ZnAl HTCs calcined at 400 °C, in which the term combined refers to the sum of chemical and physical adsorption. The adsorption capacities were lower than 1 mmol g^{-1}, in accordance with Choi et al. (2009).

Table 2 Amount of basic sites (in μmol g^{-1}) from TPD-CO_2 experiments with Mg–Al and Zn–Al HTCs calcined at 400 °C

Sample	Total amount of basic sites	Distribution of basic sites[a]		
		Weak	Medium	Strong
MgAl020	221	24 (10.8)	55 (24.9)	142 (64.3)
MgAl028	208	32 (15.4)	58 (27.9)	118 (56.7)
MgAl033	187	24 (12.8)	56 (29.9)	107 (57.3)
ZnAl020	185	35 (18.9)	21 (11.3)	129 (69.8)
ZnAl028	171	21 (12.3)	4 (2.3)	146 (85.4)
ZnAl033	150	22 (14.7)	7 (4.7)	121 (80.6)

[a] The number in parentheses is the corresponding percentage from total amount of basic sites

Table 3 CO_2 adsorption capacity at 50 °C for Mg–Al and Zn–Al HTCs calcined at 400 °C

Sample	CO_2 adsorption capacity (mmolg^{-1})			Reversible fraction (%)
	Combined	Physical	Chemical	
MgAl020	0.68	0.58	0.10	85.3
MgAl028	0.87	0.73	0.14	83.9
MgAl033	0.91	0.62	0.29	68.1
ZnAl020	0.15	0.13	0.02	86.7
ZnAl028	0.12	0.11	0.01	91.7
ZnAl033	0.21	0.18	0.03	85.7

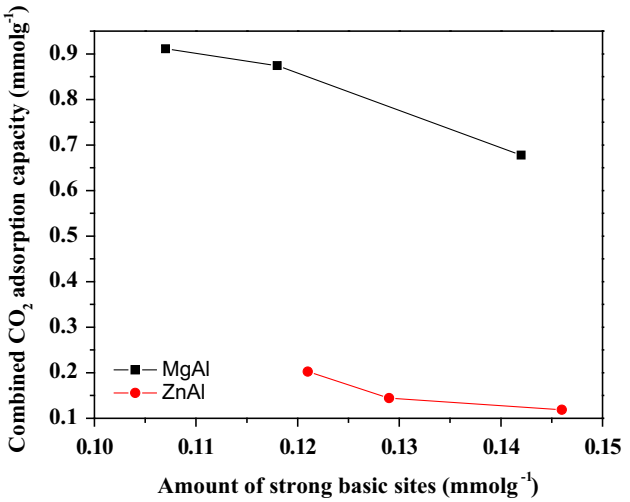

Fig. 4 Combined CO_2 adsorption capacities as a function of strong basic sites

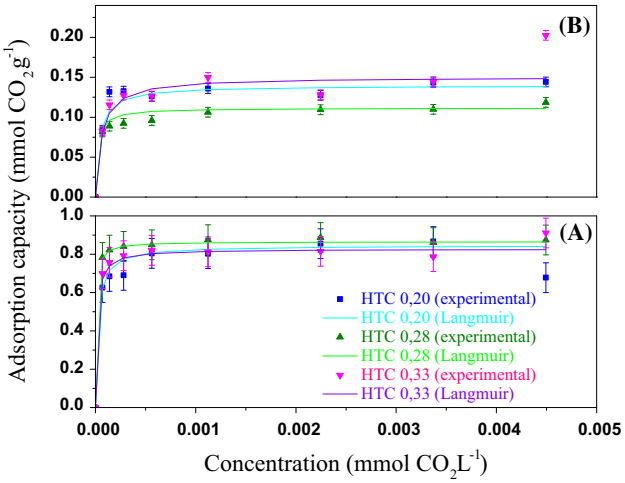

Fig. 5 CO_2 adsorption isotherms for **a** MgAl and **b** ZnAl calcined samples

The much higher CO_2 adsorption capacities of MgAl samples when compared to ZnAl can be related to their larger surface area (Table 1) and higher number of basic sites (Table 2). When analyzing MgAl or ZnAl series separately, the combined adsorption capacities do not follow the total number of basic sites. For MgAl series, the highest adsorption capacity was presented by the sample with lower amount of strong basic sites (x = 0.33), which shows that the presence of weak and medium basic sites are more important for CO_2 adsorption in this case. The correlation between CO_2 adsorption capacity and the amount of strong basic sites is shown in Fig. 4. Yong et al. (2001, 2002) observed that increasing the Al^{3+} content on Mg–Al HTs is favorable for CO_2 adsorption due to the increase of the layer charge density in HTCs and the reduction of high strength basic sites. Sharma et al. (2008) also showed that CO_2 chemisorption capacity of Mg–Al HTs increases with Al content; the maximum adsorption capacity (0.91 mmol g^{-1} at 30 °C) was obtained with x = 0.37.

For ZnAl series, the sample with the highest combined CO_2 adsorption capacity was also that with x = 0.33, which can be associated not only to its lower number of strong basic sites but also to its much higher surface area. Comparing both series, the reversible fractions were higher for ZnAl samples, especially for x = 0.33, showing that substitution of Mg^{2+} by Zn^{2+} favors physisorption over chemisorption. For MgAl samples it was observed by Torres-Rodríguez et al. (2011) formation of $MgCO_3$ after CO_2 adsorption, which explains the enhanced contribution of chemisorption.

Tsuji et al. (1993) measured a CO_2 adsorption capacity of 0.6 mmol g^{-1} at 25 °C for Mg–Al HT (x = 0.45) calcined at 400 °C, and 0.14 $mmolg^{-1}$ for Zn–Al HTC (x = 0.45) calcined at 200 °C. The CO_2 adsorption capacity at 50 °C reported by Léon et al. (2010) for Mg–Al HT (x = 0.25) calcined at 450 °C was 0.96 mmol g^{-1}. Hutson et al. (2004) measured the adsorption capacity at 200 °C: 0.9 mmol g^{-1} for Mg–Al HT (x = 0.25) calcined at 400 °C; the reversible fraction was 81.6 %. At the same adsorption temperature and the same HT composition and calcination, Wang et al. (2012) obtained an adsorption capacity of 0.58 mmol g^{-1}. Thus, the adsorption capacities obtained here are coherent with other values in the literature.

The measured adsorption isotherms were fitted into Langmuir model, as shown in Fig. 5, while Table 4 presents the Langmuir parameters. According to the correlation coefficients (R^2), it was observed that the Langmuir model fitted relatively well to the experimental points. Experimental error was calculated performing triplicates for MgAl sample with x equal to 0.28 and ZnAl with x equal to 0.20 in the CO_2 concentration of 2.25 and 0.28 mmol L^{-1}, respectively. Two other models were also tested, Freundlich and Temkin, but they failed to fit with the experimental data.

The q_m parameter for MgAl samples did not show the expected behavior when compared to CO_2 adsorption capacity (Table 3). The expected behavior was that the sample with highest adsorption presented the highest value for q_m, and this divergence is probably due to the high experimental error (8.7 %). ZnAl samples showed the expected behavior for the q_m parameter.

Ding and Alpay (2000, 2001) showed that CO_2 adsorption equilibrium on Mg–Al HTC, in both dry and wet conditions at 400–450 °C, could be adequately described by the Langmuir model. On the other hand, Sharma et al. (2008) observed that the Freundlich isotherm gave the best fit with the experimental data of CO_2 adsorption on Mg–Al HT at 30 °C.

Table 4 Langmuir parameters for CO_2 adsorption at 50 °C on Mg–Al and Zn-Al HTCs calcined at 400 °C

Sample	b (L mmol CO_2^{-1})	q_m (mmol CO_2 g^{-1})	R^2
MgAl020	38,052.44 ± 4234.40	0.84504 ± 0.01620	0.941
MgAl028	133,065.39 ± 10,150.89	0.86570 ± 0.00333	0.972
MgAl033	78,485.67 ± 4604.65	0.82688 ± 0.00415	0.983
ZnAl020	21,216.03 ± 1786.14	0.13963 ± 0.00325	0.966
ZnAl028	36,124.91 ± 4891.34	0.11146 ± 0.00272	0.915
ZnAl033	18,341.27 ± 2027.06	0.15018 ± 0.00607	0.942

Table 5 CO_2 adsorption fraction after the second and third adsorption/desorption cycles

Sample	F_2 (%)[a]	F_3 (%)[a]
MgAl020	82.1	78.8
MgAl028	77.3	72.5
MgAl033	83.0	74.7
ZnAl020	82.5	80.0
ZnAl028	70.4	66.2
ZnAl033	78.9	68.7

[a] Calculated in the relation of the first adsorption cycle

Cyclic adsorption/desorption experiments showed that the adsorption capacity decreases with increasing the number of cycles (Table 5). The adsorption fraction in the third cycle follows the order $x = 0.28 < 0.33 < 0.20$, which shows that samples with $x = 0.20$ have greater resistance to the deactivation of adsorption sites as a function of cycle number.

A possible explanation for the decrease of the CO_2 adsorption capacity in cyclic experiments is the increase of irreversible chemisorption, which decreases the amount of the sites able to CO_2 adsorption (Yong and Rodrigues 2002; Du et al. 2010; León et al. 2010). Kim et al. (2004) showed that Mg–Al HT reached a steady-state behavior for CO_2 adsorption at 150 °C after the 9th cycle. As MgAl adsorbents have higher chemical adsorption fraction (Table 3) it was expected a higher decrease in adsorption capacity of these samples with cycle number, but this was only true for $x = 0.20$ (although the difference in this case is very small). Thus, MgAl samples are more resistant to deactivation with adsorption/desorption cycles and more adequate for long-term use.

4 Conclusions

Mg–Al and Zn–Al hydrotalcite-like compounds were synthesized by coprecipitation and obtained as pure phases, as demonstrated by the XRD analyses. The calcination of adsorbents at 400 °C formed mixed oxides with the desirable basic sites responsible for the CO_2 adsorption, and increase in the specific surface area. The increase in Al content decreased the number of basic sites. Mg–Al and Zn–Al samples with Al molar composition of 0.33 showed greater CO_2 adsorption capacity at 50 °C: 0.91 and 0.21 mmol g^{-1}, respectively. Langmuir isotherm fitted well to the experimental data, since the correlation coefficients showed satisfactory values. CO_2 adsorption/desorption cycles showed that the adsorption decreases with the increasing number of cycles, demonstrating that there is deactivation due to irreversible chemisorption. When comparing the samples, it becomes clear that the adsorbent that presented the best characteristics to adsorb CO_2 was Mg–Al.

References

Abelló, S., Medina, F., Tichit, D., Pérez-Ramírez, J., Groen, J.C., Sueiras, J.E., Salagre, P., Cesteros, Y.: Aldol condensations over reconstructed Mg–Al hydrotalcites: structure–activity relationships related to the rehydration method. Chem. A. Eur. J. **11**, 728–739 (2005)

Béres, A., Pálinkó, I., Kiricsi, I., Nagy, J.B., Kiyozumi, Y., Mizukami, F.: Layered double hydroxides and their pillared derivatives – materials for solid base catalysis; synthesis and characterization. Appl. Catal. A **182**, 237–247 (1999)

Bolognini, M., Cavani, F., Scagliarini, D., Flego, C., Perego, C., Saba, M.: Heterogeneous basic catalysts as alternatives to homogeneous catalysts: reactivity of Mg/Al mixed oxides in the alkylation of m-cresol with methanol. Catal. Today **75**, 103–111 (2002)

Cavani, F., Trifiro, F., Vaccari, A.: Hydrotalcite-type anionic clays: preparation, properties and applications. Catal. Today **11**, 173–301 (1991)

Choi, S., Drese, J.H., Jones, C.W.: Adsorbent materials for carbon dioxide capture from large anthropogenic point sources. ChemSusChem **2**, 796–854 (2009)

Corma, A., Iborra, S., Primo, J., Rey, F.: One-step synthesis of citronitril on hydrotalcite derived base catalysts. Appl. Catal. A **114**, 215–225 (1994)

Corma, A., Hamid, S.B.A., Iborra, S., Velty, A.: Lewis and Brönsted basic active sites on solid catalysts and their role in the synthesis of monoglycerides. J. Catal. **234**, 340–347 (2005)

D'Alessandro, D.M., Smit, B., Long, J.R.: Carbon dioxide capture: prospects for new materials. Angew. Chem. Int. Ed. **49**, 6058–6082 (2010)

Di Cosimo, J.I., Díez, V.K., Xu, M., Iglesia, E., Apesteguia, C.R.: Structure and surface and catalytic properties of Mg-Al basic oxides. J. Catal. **178**, 499–510 (1998)

Ding, Y., Alpay, E.: Equilibria and kinetics of CO_2 adsorption on hydrotalcite adsorbent. Chem. Eng. Sci. **55**, 3461–3474 (2000)

Ding, Y., Alpay, E.: High temperature recovery of CO_2 from flue gases using hydrotalcite adsorbent. Trans. IChemE **79**, 45–51 (2001)

Du, H., Ebner, A.D., Ritter, J.A.: Temperature dependence of the nonequilibrium kinetic model that describes the adsorption and desorption behavior of CO_2 in K-promoted HTlc. Ind. Eng. Chem. Res. **49**, 3328–3336 (2010)

Hutson, N.D., Speakman, S.A., Payzant, E.A.: Structural effects on the high temperature adsorption of CO_2 on a synthetic hydrotalcite. Chem. Mater. **16**, 4135–4143 (2004)

Hutson, N.D., Attwood, B.C.: High temperature adsorption of CO_2 on various hydrotalcite-like compounds. Adsorption **14**, 781–789 (2008)

International Energy Agency: CO_2 emissions from fuel combustion highlights, www.iea.org. Accessed Sept 2014

Kim, Y., Yang, W., Liu, P.K.T., Sahimi, M., Tsotsis, T.T.: Thermal evolution of the structure of a Mg-Al-CO_3 layered double hydroxide: sorption reversibility aspects. Ind. Eng. Chem. Res. **43**, 4559–4570 (2004)

Kustrowski, P., Chmielarz, L., Bozek, E., Sawalha, M., Roessner, F.: Acidity and basicity of hydrotalcite derived mixed Mg–Al oxides studied by test reaction of MBOH conversion and temperature programmed desorption of NH_3 and CO_2. Mater. Res. Bull. **39**, 263–281 (2004)

Kustrowski, P., Sułkowska, D., Chmielarz, L., Rafalska-Łasocha, A., Dudek, B., Dziembaj, R.: Influence of thermal treatment conditions on the activity of hydrotalcite-derived Mg–Al oxides in the aldol condensation of acetone. Microp. Mesop. Mater. **78**, 11–22 (2005)

León, M., Díaz, E., Bennici, S., Vega, A., Ordóñez, S., Auroux, A.: Adsorption of CO_2 on hydrotalcite-derived mixed oxides: sorption mechanisms and consequences for adsorption irreversibility. Ind. Eng. Chem. Res. **49**, 3663–3671 (2010)

Liu, Q., Wang, B., Wang, C., Tian, Z., Qu, W., Ma, H., Xu, R.: Basicities and transesterification activities of Zn–Al hydrotalcites-derived solid bases. Green Chem. **16**, 2604–2613 (2014)

Oliveira, E.L.G., Grande, C.A., Rodrigues, A.E.: CO_2 sorption on hydrotalcite and alkali-modified (K and Cs) hydrotalcites at high temperatures. Sep. Purif. Technol. **62**, 137–147 (2008)

Ram Reddy, M.K., Xu, Z.P., Lu, G.Q., Costa, J.C.D.: Layered double hydroxides for CO_2 capture: structure evolution and regeneration. Ind. Eng. Chem. Res. **45**, 7504–7509 (2006)

Rodrigues, A.C.C.: Influence of the composition on the electronegativity and on the oxygen charge distribution in a binary hydrotalcite-like by modified Sanderson method. J. Math. Chem. **37**, 347–351 (2005)

Sampieri, A., Lima, E.: On the acid-base properties of microwave irradiated hydrotalcite-like compounds containing Zn^{2+} and Mn^{2+}. Langmuir **25**, 3634–3639 (2009)

Sharma, U., Tyagi, B., Jasra, R.V.: Synthesis and characterization of Mg-Al-CO_3 layered double hydroxide for CO_2 adsorption. Ind. Eng. Chem. Res. **47**, 9588–9595 (2008)

Silva, C.C.C.M., Ribeiro, N.F.P., Souza, M.M.V.M., Aranda, D.A.G.: Biodiesel production from soybean oil and methanol using hydrotalcites as catalyst. Fuel Process. Technol. **91**, 205–210 (2010)

Sing, K.S.W., Everett, D.H., Haul, R.A.W., Moscou, L., Pierotti, R.A., Rouquerol, J., Siemieniewska, T.: Reporting physisorption data for gas/solid system with special reference to the determination of surface area and porosity. Pure Appl. Chem. **57**, 603–619 (1985)

Torres-Rodríguez, D.A., Lima, E., Valente, J.S., Pfeiffer, H.: CO_2 capture at low temperatures (30–80°C) and in the presence of water vapor over a thermally activated Mg-Al layered. J. Phys. Chem. A **115**, 12243–12250 (2011)

Tsuji, M., Mao, G., Yoshida, T., Tamaura, Y.: Hydrotalcites with an extended Al^{3+}-substitution: synthesis, simultaneous TG-DTA-MS study, and their CO_2 adsorption behaviors. J. Mater. Res. **8**, 1137–1142 (1993)

Wang, Q., Luo, J., Zhong, Z., Borgna, A.: CO_2 capture by solid adsorbents and their applications: current status and new trends. Energy Environ. Sci. **4**, 42–55 (2011)

Wang, Q., Tay, H.H., Guo, Z., Chen, L., Liu, Y., Chang, J., Zhong, Z., Luo, J., Borgna, A.: Morphology and composition controllable synthesis of Mg–Al–CO_3 hydrotalcites by tuning the synthesis pH and the CO_2 capture capacity. Appl. Clay Sci. **55**, 18–26 (2012)

Yang, W., Kim, Y., Liu, P.K.T., Sahimi, M., Tsotsis, T.T.: A study by in situ techniques of the thermal evolution of the structure of a Mg–Al–CO_3 layered double hydroxide. Chem. Eng. Sci. **57**, 2945–2953 (2002)

Yong, Z., Mata, V., Rodrigues, A.E.: Adsorption of carbon dioxide onto hydrotalcite-like compounds (HTLCs) at high temperatures. Ind. Eng. Chem. Res. **40**, 204–209 (2001)

Yong, Z., Rodrigues, A.E.: Hydrotalcite-like compounds as adsorbents for carbon dioxide. Energy Convers. Manag. **43**, 1865–1876 (2002)